

# Enhanced Study and Control of Analyte Oxidation in Electrospray Using a Thin-Channel, Planar Electrode Emitter

Gary J. Van Berkel,\* Keiji G. Asano, and Vilmos Kertesz†

Organic and Biological Mass Spectrometry Group, Chemical Sciences Division, Oak Ridge National Laboratory, Oak Ridge, Tennessee 37831-6365

**A thin-channel, planar electrode emitter device is described and utilized for the study and control of electrochemical oxidation of analytes at the emitter electrode in an electrospray ion source. For analytes that are not particularly susceptible to oxidation, the planar electrode device functions analytically in a manner similar to emitter systems that utilize the more common stainless steel tubular electrodes. For more easily oxidized analytes, the device provides the means to achieve near 100% oxidation efficiency or to completely eliminate analyte oxidation through simple and rapid changes in electrode material, electrode area, electrode covering, channel height above the electrode, or solution flow rate. Compared to the use of tubular electrodes, the planar electrode emitter system provides improved flexibility in altering the nature of the electrode area and material, as well as altering analyte mass transport to the electrode surface. Each of these parameters is critical in the control of electrochemical reactions and can be easily studied or exploited with this emitter electrode configuration.**

The typical electrospray (ES) ion source used in mass spectrometry (MS) is a two-electrode, controlled-current electrochemical flow cell.<sup>1–5</sup> A metal capillary or other conductive contact (usually stainless steel) placed at or near the point from which the charged ES droplet plume is generated (the ES emitter) is one of two electrodes in the system. The analytically significant reactions in terms of ES-MS occur at this electrode acting as the working electrode in the system.<sup>5</sup> The counter electrode of the circuit is usually the atmospheric sampling aperture plate or inlet capillary and the various lens elements and detector of the mass spectrometer.<sup>6</sup> To sustain the production of charged droplets from

the ES source, electrochemical reactions must occur at the conductive contact to the solution at the spray end of the ES device. Oxidation reactions in positive ion mode and reduction reactions in negative ion mode dominate at the emitter electrode, whereas reduction reactions in positive ion mode and oxidation reactions in negative ion mode dominate at the counter electrode.

In as much as the specific analyte ions and their respective abundances observed in an ES mass spectrum are related to solution composition,<sup>7,8</sup> the electrochemical reactions that take place at the ES emitter electrode may influence the gas-phase ions formed and ultimately analyzed by the mass spectrometer. This is because the electrochemical reactions at the emitter electrode can change the composition of the solution that initially enters the ES ion source.<sup>9</sup> Of particular interest are those electrochemical reactions and compositional changes that directly involve the analytes. These reactions include electrochemical ionization that can be exploited to ionize neutral electroactive analytes that would otherwise go undetected in ES-MS.<sup>1,10,11</sup> Other reactions include those that modify the mass, structure, or charge of the analyte<sup>12</sup> and those that can remove analytes from solution.<sup>13</sup> Reactions of the latter types might be troublesome for analyses involving unknown analytes or quantification. The ability to control the extent of any or all of these analyte electrochemical reactions would be an analytical advantage.<sup>1–5</sup>

The interfacial potential at the working electrode, the magnitude of the ES current, the nature of the electrode surface, and the mass transport of the analyte to the electrode are all important parameters in determining which reactions can occur at the emitter electrode, their rates, and their extent. The interfacial potential of the ES emitter electrode, for a given applied voltage, is not fixed, but rather adjusts to a given level depending upon a number of interactive variables to provide the required current. These variables include the magnitude of the ES current, the redox character and concentrations of all species in the system,

\* Corresponding author. Phone: 865-574-1922. Fax: 865-576-8559. E-mail: vanberkelgj@ornl.gov.

† Current address: Győr, Móra Ferenc tér 14. I/3., H-9028, Hungary.

- (1) Van Berkel, G. J. The Electrolytic Nature of Electrospray. In *Electrospray Ionization Mass Spectrometry: Fundamentals, Instrumentation and Applications*; Cole, R., Ed.; John Wiley: New York, 1997; Chapter 2, pp 65–105.
- (2) de la Mora, J. F.; Van Berkel, G. J.; Enke, C. G.; Cole, R. B.; Martinez-Sanchez, M.; Fenn, J. B. *J. Mass Spectrom.* **2000**, *35*, 939–952.
- (3) Van Berkel, G. J.; Zhou, F. *Anal. Chem.* **1995**, *67*, 2916–2923.
- (4) Van Berkel, G. J.; Giles, G. E.; Bullock, J. S., IV; Gray, L. J. *Anal. Chem.* **1999**, *71*, 5288–5296.
- (5) Van Berkel, G. J. *J. Am. Soc. Mass Spectrom.* **2000**, *11*, 951–960.
- (6) Jackson, G. S.; Enke, C. G. *Anal. Chem.* **1999**, *71*, 3777–3784.

- (7) Mansoori, B. A.; Volmer, D. A.; Boyd, R. K. *Rapid Commun. Mass Spectrom.* **1997**, *11*, 1120–1130.
- (8) Zhou, S. L.; Cook, K. D. *J. Am. Soc. Mass Spectrom.* **2000**, *11*, 961–966.
- (9) Van Berkel, G. J.; Zhou, F.; Aronson, J. T. *Int. J. Mass Spectrom. Ion Processes* **1997**, *162*, 55–62.
- (10) Van Berkel, G. J.; McLuckey, S. A.; Glish, G. L. *Anal. Chem.* **1992**, *64*, 1586–1593.
- (11) Van Berkel, G. J.; Zhou, F. *Anal. Chem.* **1995**, *67*, 3958–3964.
- (12) Karancsi, T.; Slegel, P.; Novak, L.; Pirok, G.; Kovacs, P.; Vekey, K. *Rapid Commun. Mass Spectrom.* **1997**, *11*, 81–84.
- (13) Van Berkel, G. J. *J. Mass Spectrom.* **2000**, *35*, 773–783.

the solution flow rate, the electrode material, geometry, and area, and any other parameters that affect the flux of reactive species to the electrode surface.<sup>1,3–5</sup> The current magnitude limits the extent or efficiency of the reactions. We have investigated the experimental means to alter ES current (e.g., by addition of electrolyte) and have investigated the effect of different types and lengths of metal tubular electrodes (e.g., stainless steel, platinum, and copper tubes) on the extent of oxidation of various analytes in the ES emitter.<sup>3,10,11,14,15</sup> However, the basic tubular electrode design presents limited means to alter the electrode material and area and, more generally, mass transport to the electrode. In tubular electrode emitter designs, the emitter electrode and emitter spray tip are one. The inner and outer dimensions of the tube, and therefore, electrode geometry, area, and mass transport distances, are restricted to a small range that provides a quality spray. In addition, a limited number of conductive materials are commercially available in tubular form of the appropriate dimensions. This limits the materials that can be used as electrodes. Moreover, tubular electrodes are easily plugged or damaged and, therefore, depending on the material, can be an expensive consumable (e.g., platinum capillaries).<sup>11</sup>

We describe in this paper a thin-channel, planar electrode ES emitter device in which the electrode and a nonconductive emitter spray tip are separated. This configuration allows electrode area, electrode material, electrode covering, and flow path channel height (or width) to be rapidly and conveniently changed. This provides greater opportunity to control mass transport to the electrode surface while more fully exploiting the known role of electrode material in influencing electrochemical reactions,<sup>16</sup> without negatively impacting spray quality. The data presented demonstrate for nonelectroactive analytes that the analytical performance of this ES ion source is very similar to traditional ES ion sources that use tubular electrodes. For more easily oxidized analytes, the device is shown to provide the means to easily alter the extent of analyte oxidation from near 100% to an insignificant fraction of the total amount of material flowing through the system. Furthermore, the data demonstrate the major influence electrode material and ES current magnitude can have on the extent of analyte oxidation.

## EXPERIMENTAL SECTION

**Samples and Reagents.** Bovine insulin (Sigma, St. Louis, MO), dopamine (Aldrich, Milwaukee, WI), *N*-phenyl-1,4-phenylenediamine (Aldrich), and the polypropylene glycol tuning solution (MDS Sciex, Concord, ON, Canada) were used as received. Analyte solutions were prepared just prior to analysis to minimize any oxidation by exposure to air and light. *N*-Phenyl-1,4-phenylenediamine and dopamine solutions were prepared in a 1/1 (v/v) mixture of water (Milli-RO 12 Plus, Bedford, MA) and methanol (Burdick and Jackson, Muskegon, MI) containing 0.75% (v/v) acetic acid (HOAc, PPB/Teflon grade, Aldrich) and 5.0 mM ammonium acetate (NH<sub>4</sub>OAc, 99.999%, Aldrich). The bovine insulin solution was prepared in 1/1 (v/v) water/acetonitrile (Burdick and Jackson) containing 0.1% (v) HOAc.

(14) Kertesz, V.; Van Berkel, G. J. *J. Mass Spectrom.* **2001**, *36*, 204–210.

(15) Van Berkel, G. J.; Kertesz, V. *J. Mass Spectrom.* **2001**, *36*, 1125–1132.

(16) *Laboratory Techniques in Electroanalytical Chemistry*; Kissinger, P. T., Heineman, W. R., Eds.; Marcel Dekker: New York, 1996.

**ES-MS.** ES-MS experiments were performed on either a PE Sciex API 365 triple quadrupole or API 165 single quadrupole mass spectrometer (MDS Sciex). Solvent flow through the ES systems in all cases was provided by a syringe pump or gas displacement pump. Sample was introduced to the ion source by either continuous infusion or by flow injection using a variable-volume loop injector (Rheodyne model 7125, Cotati, CA). Experiments with a normal capillary ES emitter were performed with a TurboIonSpray ES ion source using a 3.5-cm-long stainless steel capillary (MDS Sciex, 0.4 mm o.d. × 0.1 mm i.d.). No “turbo” gas was used. In other experiments, the TurboIonSpray ES ion source was removed and replaced with a thin-channel, planar electrode, ES emitter device (Figure 1). This device used the source housing and *x*, *y*, *z* positioner of a Protana NanoES source (Protana A/S, Odense, Denmark) designed for use with the Sciex instruments. With this arrangement, all instrument safety interlocks remained active. The planar electrode device was electrically isolated from upstream components using a grounded stainless steel union. The ES current was measured by grounding the curtain plate (normally 1.0 kV) of the mass spectrometer through a Keithley model 610C electrometer (Cleveland, OH) and lowering the emitter electrode voltage by 1.0 kV. The spray capillary was moved laterally beyond the sampling orifice so all of the charged droplets impacted the curtain plate.

The planar electrode ES emitter device was composed of three major components, viz., an inlet/outlet block fashioned from PEEK, a Teflon spacing gasket that defined the channel height (and width), and a PEEK electrode block in which was embedded a disk electrode. The latter two items were the same components as those used in the cross-flow, thin-layer electrochemical flow cell that is commercially available from Bioanalytical Systems, Inc. (BAS, West Lafayette, IN). The PEEK inlet/outlet block was fashioned largely after the stainless steel auxiliary electrode block of the BAS cell, including electrode and gasket alignment pins and the hand-tightened screw that provides a means to secure a leak-proof seal. However, our inlet/outlet block was fashioned with smaller bore through holes (250 μm) and did not contain a reference electrode port. The particular electrodes used in this study were disk electrodes offset from center (electrode edge at block center line): 6.0-mm-diameter glassy carbon (GC); dual 6.0-mm GC; 3.0-mm GC; 6.3-mm platinum; 6.0-mm silver; 6.0-mm copper; 6.0-mm zinc; and 6.0-mm 316L stainless steel. Spacing gaskets used were 13, 51, and 127 μm thick providing cell volumes above a 6.0-mm-diameter electrode of approximately 0.5, 1.9, and 4.9 μL, respectively. Solution exited the device and was sprayed through a 3.5-cm length of 50-μm-i.d., 360-μm-o.d. fused-silica capillary with a TaperTip (New Objective, Inc., Woburn, MA). This capillary was held in place using a 1/16-in.-o.d. Teflon sleeve, a PEEK ferrule, and the nebulizer tube from the TurboIonSpray source. A small-gauge tube was welded to the nebulizer tube to allow connection of the nebulizing gas supply to pneumatically assist the ES process. Prior to all experiments, the electrodes were freshly polished. In some experiments, a cellulose ester 5000 Da molecular mass cutoff membrane (Sialomed, Inc., Columbia, MD) was used to cover the working electrode.

## RESULTS AND DISCUSSION

**Planar Electrode Emitter Setup and Operation with Nonelectroactive Analytes.** A schematic illustration of the thin-

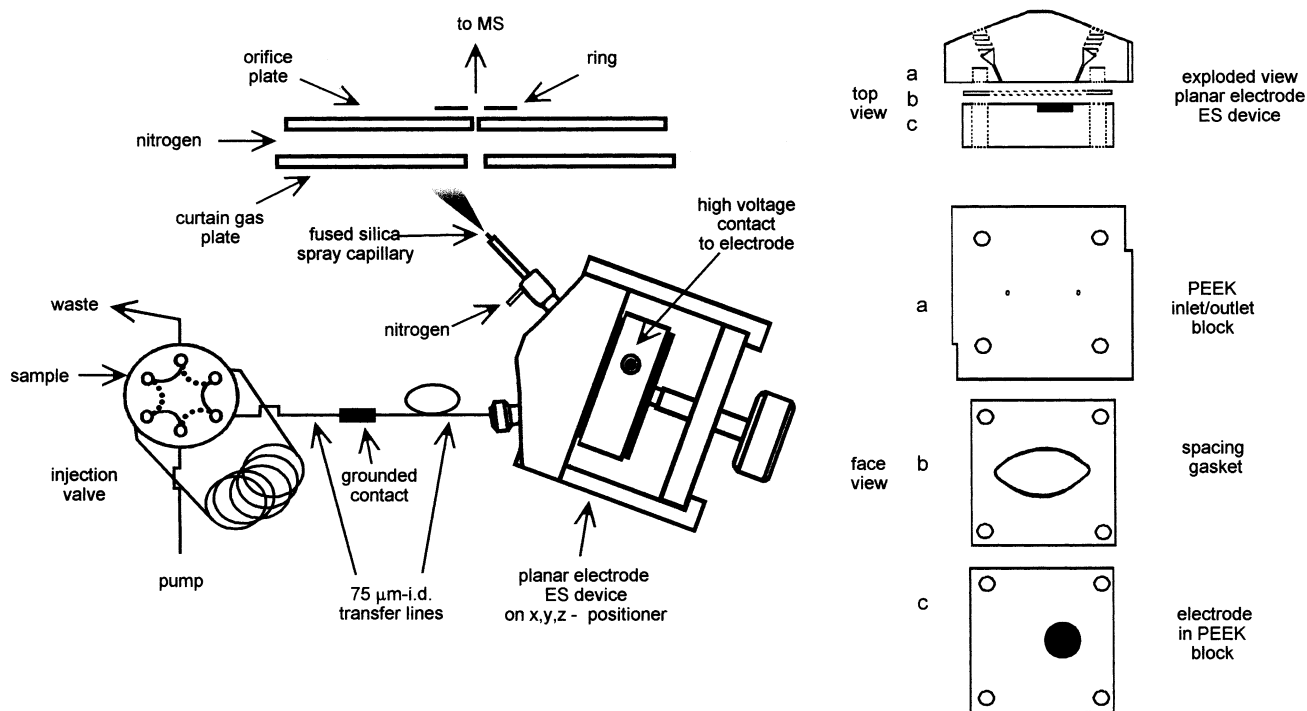


Figure 1. Schematic illustration of the planar electrode ES emitter setup. Exploded view is drawn to scale.

channel, planar electrode ES emitter device is shown in Figure 1. The high-voltage contact to solution was provided via an interchangeable planar electrode in a PEEK block upstream of the spray tip. This electrode was positioned between the inlet and outlet port of another block and separated from that block by a spacing gasket, providing a thin-layer flow channel over the electrode. The volume of the cell and the mass transport characteristics of the device were altered by varying any of the following: electrode area, electrode covering, spacing gasket thickness, and solution flow rate. The electrode material was altered by using different electrodes in discrete blocks, and the electrode area was varied by using electrodes of different diameter. Though not demonstrated here, it is also possible to alter the electrode area by changing the shape of the cutout in the spacing gasket. The solution exited the device and was sprayed from a nonconductive fused-silica capillary with pneumatic nebulization to enhance gas-phase ion formation at higher solution flow rates. For the experimental results shown here, sample was often directly infused through the emitter, but an injection valve added to the system allowed flow injection experiments. Spraying the eluate from a separation device such as an HPLC would be accomplished by a simple change in plumbing, coupling the column to the grounded contact.

For compounds not particularly prone to electrochemical oxidation, this device performed in an analytical fashion similar to our commercial pneumatically assisted ES ion source, which makes use of a stainless steel tubular electrode emitter. For example, using the polypropylene glycol solution supplied with the instrument for mass-to-charge calibration, no significant difference among the spectra acquired with the commercial source and the planar electrode emitter device was observed (data not shown). The mass measured for the polypropylene glycol ions was the same in each spectrum ( $\pm 0.1 m/z$ ) and their respective intensities among experiments differed by no more than  $\sim 20\%$ .

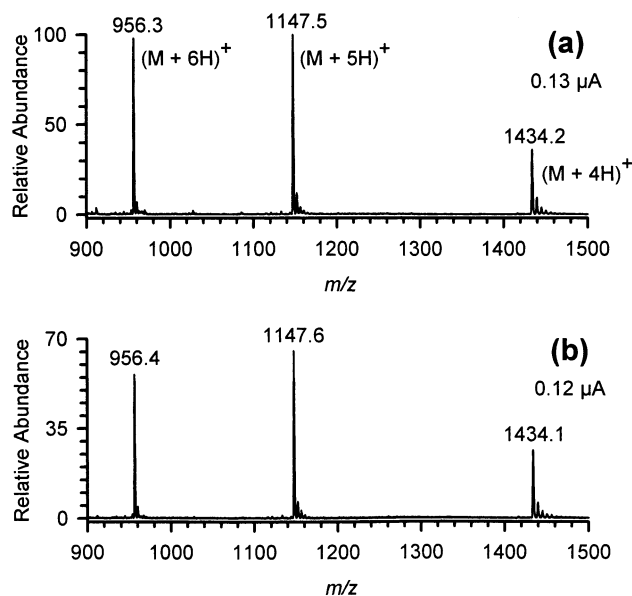
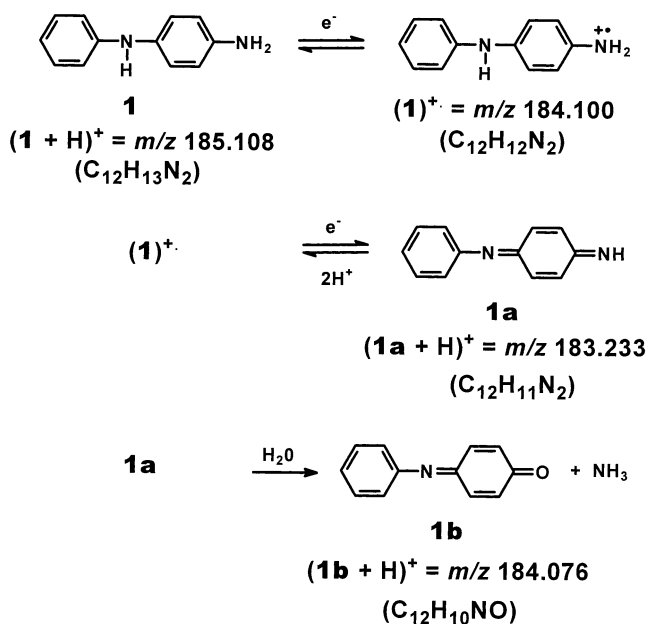


Figure 2. Mass spectra acquired from a  $1.7 \mu\text{M}$  solution of bovine insulin (1/1 v/v water/acetonitrile, 0.1% (v) HOAc) using (a) the normal TurbolonSpray source with a 304 stainless steel capillary emitter electrode and (b) the planar electrode emitter device with a 6.0-mm-diameter 316L stainless steel electrode. The tip of the emitter spray capillary was placed in approximately the same position for each experiment, and the solution flow rate ( $10 \mu\text{L}/\text{min}$ ) and applied voltage (4.5 kV) were the same in both cases. The nebulizing gas setting for optimum performance in the two cases was slightly different.

To further illustrate, the data in Figure 2 were acquired using the protein bovine insulin as the analyte ( $M_r \text{ calcd} = 5733.6 \text{ Da}$ ). The spectrum in panel a was obtained using the commercial stainless steel tubular electrode emitter system, and the spectrum in panel b was obtained using a stainless steel disk electrode in the planar electrode device. The three major insulin ions observed

Scheme 1



and the deconvoluted molecular mass was the same for each spectrum ( $M_{r, \text{measd}} = 5733.0$  Da or  $\sim 0.6$  Da (0.01%) below the calculated value). The only difference in the spectra was the  $\sim 30\%$  lower intensity of the signal in the case of the planar electrode device. Conditions between the two emitter systems were nearly identical. Independent optimization of the parameters among emitters (e.g., nebulization gas flow, ES high voltage, or sprayer position) can be expected to better equalize performance. In our experience, the planar electrode system, and upstream electrode configurations in general,<sup>10,13</sup> operate better with applied electrode voltages slightly higher than needed when spraying from a metal capillary electrode. This phenomenon may relate to the voltage drop through solution in the upstream electrode system.<sup>6</sup>

**Operation with Electroactive Analytes.** In the analysis of species that are more prone to oxidation, the planar electrode system provides great flexibility in altering the nature of the electrode area and material, as well as altering analyte mass transport to the electrode surface, each of which can be an important factor in the control of electrochemical reactions.<sup>16</sup> We carried out a series of experiments with *N*-phenyl-1,4-phenylenediamine and dopamine to study the influence of these variable parameters on the extent of oxidation at the ES emitter electrode.

**Effect of Electrode Material and Flow Rate.** The ES mass spectra in Figure 3 show the molecular ion region for *N*-phenyl-1,4-phenylenediamine (**1**) obtained spraying a  $20 \mu\text{M}$  solution from the planar electrode emitter system with five different emitter electrodes at six different flow rates. This compound can undergo a two-step electrochemical oxidation forming first the cation radical, **(1)<sup>•+</sup>**, and subsequently *N*-phenyl-1,4-phenylenediamine (**1a**). This latter species may then undergo a relatively slow hydrolysis to form the quinone **1b** (Scheme 1).<sup>14,15,17</sup> Consequently, the molecular ion region can show up to four different species, depending on the extent of oxidation and hydrolysis, which appear at  $m/z$  183, 184, and 185. This molecular ion region

Table 1. Calculated ES Current Required for 100% Oxidation of **1** to **1a** and the Measured  $i_{\text{ES}}$  Values for the Various Experiments Shown in Figure 3

flow rate ( $\mu\text{L}/\text{min}$ )	$i_{\text{ES}}$ required for 100% oxidation ( $\mu\text{A}$ ) <sup>a</sup>	$i_{\text{ES}}$ measured ( $\mu\text{A}$ ) <sup>b</sup>				
		Pt	GC	Ag	Cu	Zn
1.5	0.0965	<i>0.19</i>	<i>0.25</i>	<i>0.24</i>	<i>0.24</i>	<i>0.24</i>
2.5	0.16	<i>0.20</i>	<i>0.24</i>	<i>0.24</i>	<i>0.24</i>	<i>0.24</i>
5.0	0.32	0.22	0.26	0.26	0.24	0.26
10	0.64	0.25	0.26	0.28	0.26	0.29
15	0.965	0.25	0.28	0.30	0.28	0.30
20	1.3	0.26	0.28	0.30	0.30	0.31

<sup>a</sup>  $i_{\text{ES}}$  required =  $nFvC_A$ , where  $i_{\text{ES}}$  required is the current magnitude for oxidation of the molar equivalent of the analyte flowing through the emitter,  $n$  is the molar equivalent of electrons involved in the redox reaction of **1** to **1a** ( $n = 2$ ),  $F$  is the Faraday constant ( $9.65 \times 10^4$  C/mol),  $v$  is the volumetric flow rate through the emitter, and  $C_A$  is the bulk solution concentration of the analyte. <sup>b</sup> Values in italic type indicate  $i_{\text{ES}}$  measured >  $i_{\text{ES}}$  required. Values in roman type indicate  $i_{\text{ES}}$  measured <  $i_{\text{ES}}$  required.

is complicated by the overlap of the isotope peak of the protonated molecule of **1a** ( $^{13}\text{C}^{12}\text{C}_{11}\text{H}_{11}\text{N}_2$ ) at  $m/z$  184 with the radical cation and protonated hydrolysis product. However, visual inspection of the spectra quickly reveals whether the oxidation is relatively efficient (**(1a + H)<sup>+</sup>** at  $m/z$  183 dominant) or inefficient (**(1 + H)<sup>+</sup>** at  $m/z$  185 dominant). In the present data set, one observes that complete oxidation of **1** to **1a** was achieved using the platinum, glassy carbon, and silver electrodes at flow rates of 1.5 and 2.5  $\mu\text{L}/\text{min}$ . At higher flow rates, the extent of oxidation progressively decreased. The ability to oxidize **1** indicates that the electrode interfacial potential is near to or greater than the equilibrium potential for this reaction (Figure 4,  $E_{p/2} = 0.48$  V versus SHE).<sup>17,18</sup> The inability to completely oxidize the compound at higher flow rates is due to the limited ES current. In Table 1 are shown the calculated ES currents required for complete oxidation of **1** to **1a** along with the measured ES currents for each experiment. The currents among all electrodes at the same respective flow rates are very similar, but only at flow rates of 1.5 and 2.5  $\mu\text{L}/\text{min}$  is there more current than that required for complete oxidation. Without sufficient current, the oxidation of **1** to **1a** must be less than 100% complete, regardless of the electrode potential.

When the copper or zinc electrode was used, no oxidation of **1** was observed at any flow rate even though the current magnitude was sufficient at the lowest flow rates for complete oxidation (Figure 3 and Table 1). This is the result of a redox buffering effect caused by corrosion of the respective emitter electrodes.<sup>5,9,15</sup> Because the ES ion source operates as a controlled-current electrolytic cell, it is possible to control the interfacial potential at the electrode through the use of redox buffers. Oxidation or reduction of the redox buffer to supply the required current in the system maintains the electrode near the potential of that reaction. By appropriate selection of the working electrode material, the corrosion of the electrode in positive ion mode can be used to obtain this redox buffering effect. As illustrated in Figure 4, the potentials at which the copper and zinc electrochemically oxidize are below that necessary to oxidize **1** to **1a**; thus, the latter reaction cannot occur. Neither glassy carbon, platinum, nor silver is easily oxidized so the interfacial potential

(17) Kertesz, V.; Deng, H.; Asano, K. G.; Hettich, R. L.; Van Berkel, G. J. *Electroanalysis*, in press.

(18) Deng, H.; Van Berkel, G. J. *Anal. Chem.* **1999**, *71*, 4284–4293.

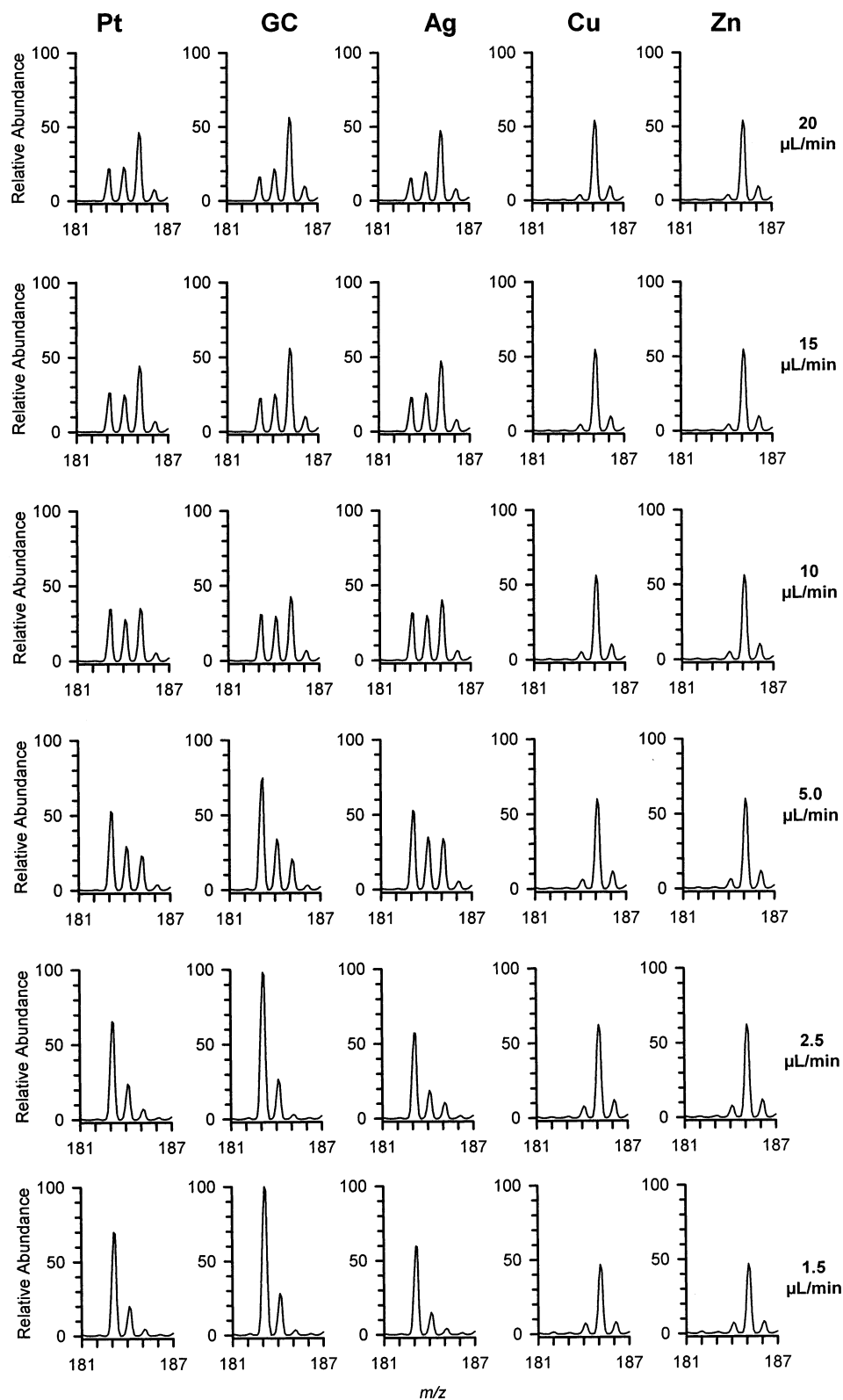


Figure 3. A series of mass spectra showing the molecular ion region for a 20  $\mu\text{M}$  solution of *N*-phenyl-1,4-phenylenediamine obtained using the planar electrode emitter device with either a Pt, GC, Ag, Cu, or Zn electrode at flow rates of 1.5, 2.5, 5.0, 10, 15, and 20  $\mu\text{L}/\text{min}$ . The tip of the emitter spray capillary was placed in the same position for each experiment, and the applied voltage (4.5 kV) and nebulizing gas settings are all identical. Ion abundances are normalized to the largest signal recorded for the molecular species among all the experiments (i.e., GC, 2.5  $\mu\text{L}/\text{min}$ ).

that is present may be above that needed for analyte oxidation, if that potential is required to supply the current demand of the system.

The data in Figure 3 illustrate that the identity of the electrode material can have a major influence on the analyte species observed. The glassy carbon electrode provided the best perfor-

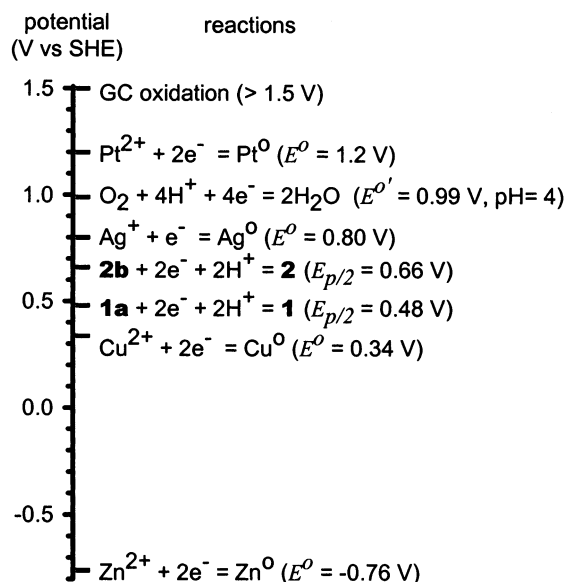


Figure 4. Potential scale showing the redox reactions relevant to this work.

mance for promoting oxidation of **1**, where the abundance of the oxidized species **1a** observed in the gas phase was significantly greater than that observed when either the platinum or silver electrode was used. The copper and zinc electrodes provided similar results with respect to suppression of the oxidation of **1**. The potential required for oxidation of each of these electrodes is less than the equilibrium potential for the oxidation of **1** to **1a**, providing a redox buffering effect (Figure 4).

**Effect of Analyte Concentration and Flow Rate.** Using the 6.0-mm-diameter glassy carbon electrode, the data in Figure 5 were gathered to study the efficiency of the oxidation of **1** to **1a** as a function of analyte concentration and solution flow rate. At the low concentration of 1.0  $\mu\text{M}$ , the efficiency of the oxidation was 100% for all flow rates studied (1.5–20  $\mu\text{L}/\text{min}$ ). At 10  $\mu\text{M}$ , the reaction remained 100% efficient up to a flow rate of 10  $\mu\text{L}/\text{min}$ . At 20  $\mu\text{M}$ , the efficiency was  $\sim$ 100% at 1.5  $\mu\text{L}/\text{min}$  but dropped below this level at higher flow rates. At 50 and 100  $\mu\text{M}$ , the oxidation was less than 100% efficient at all flow rates.

The data obtained for the 1.0  $\mu\text{M}$  solution, which shows 100% oxidation efficiency at all flow rates, indicates that mass transport to the electrode is very effective even at the high flow rates. Thus, the main reason for the oxidation efficiency drop off with increasing flow rate at higher analyte concentrations is not limited mass transport but relates to the limited ES current. In Table 2 are shown the calculated ES currents required for complete oxidation of **1** to **1a** along with the measured ES currents for each experiment as a function of analyte concentration and flow rate. The flow rate at which the oxidation is observed to be less than 100% efficient in Figure 5 correlates closely with the point at which the ES current is calculated to be less than that needed to oxidize all the material traveling through the system.

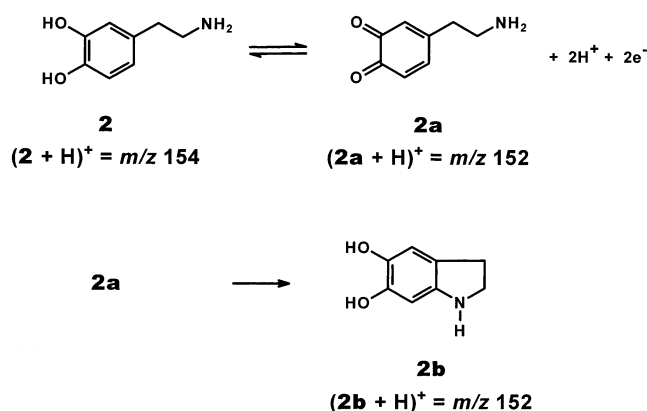
**Effect of Electrode Area, Channel Height, and Solution Flow Rate.** The role of electrode area, channel height, and solution flow rate, each of which influence mass transport to the electrode, was examined using dopamine (**2**) as a model system. The major electrochemical reaction of this analyte involves the two-electron, two-proton oxidation and intermolecular cyclization shown in

Table 2. Calculated ES Current Required for 100% Oxidation of **1** to **1a** and the Measured  $i_{\text{ES}}$  Values for the Various Experiments Shown in Figure 5

flow rate ( $\mu\text{L}/\text{min}$ )	$i_{\text{ES}}$ measured	$i_{\text{ES}}$ required ( $\mu\text{A}$ ) <sup>a</sup>				
		1.0 $\mu\text{M}$	10 $\mu\text{M}$	20 $\mu\text{M}$	50 $\mu\text{M}$	100 $\mu\text{M}$
1.5	0.25	<i>0.0048</i>	<i>0.048</i>	<i>0.096</i>	<i>0.24</i>	<i>0.48</i>
2.5	0.25	<i>0.0080</i>	<i>0.080</i>	<i>0.16</i>	<i>0.40</i>	<i>0.80</i>
5.0	0.26	<i>0.016</i>	<i>0.16</i>	0.32	0.80	1.6
10	0.265	<i>0.032</i>	0.32	0.64	1.6	3.2
15	0.28	<i>0.048</i>	0.48	0.97	2.4	4.8
20	0.285	<i>0.064</i>	0.64	1.3	3.2	6.4

<sup>a</sup>  $i_{\text{ES}}$  required =  $nFvC_A$ , where  $i_{\text{ES}}$  required is the current magnitude for oxidation of the molar equivalent of the analyte flowing through the emitter,  $n$  is the molar equivalent of electrons involved in the redox reaction of **1** to **1a** ( $n = 2$ ),  $F$  is the Faraday constant ( $9.65 \times 10^4$  C/mol),  $v$  is the volumetric flow rate through the emitter, and  $C_A$  is the bulk solution concentration of the analyte. Values in italic type indicate  $i_{\text{ES}}$  measured  $>$   $i_{\text{ES}}$  required. Values in roman type indicate  $i_{\text{ES}}$  measured  $<$   $i_{\text{ES}}$  required.

Scheme 2



Scheme 2.<sup>19</sup> Dopamine is observed as the protonated molecule,  $(\mathbf{2} + \text{H})^+$ , in the ES mass spectrum at  $m/z$  154, while the protonated molecule of the oxidized product,  $(\mathbf{2b} + \text{H})^+$ , is observed at  $m/z$  152. The ratio of the intensity of the oxidized product to the sum of the intensity of the oxidized and reduced species,  $(I_{152}/I_{(152+154)})$  plotted in Figure 6a, was used to express the extent of oxidation of this analyte (1.0 = 100% oxidized; 0 = 0% oxidized) under the different conditions. Plotted in Figure 6b is the ES current magnitude in excess of that necessary for complete oxidation of **2** to **2b** in the corresponding experiments. Negative values for the current excess indicate that the measured current (an average of  $\sim$ 0.75  $\mu\text{A}$  among experiments) was less than that necessary to oxidize all the analyte flowing through the system.

The 3.0-mm GC electrode was smaller than the width of the spacing gasket so a substantial fraction of the material passing through the cell could be as much as 1.0 mm away from the electrode, regardless of the gasket thickness. This resulted in only  $\sim$ 50% of the material being oxidized under the best conditions. As gasket thickness or flow rate was increased, the fraction of material oxidized was further diminished. The exception was the small increase in the extent of oxidation at 5.0 and 10  $\mu\text{L}/\text{min}$  with the 13- $\mu\text{m}$  gasket. Interestingly, this same trend is seen

(19) Deng, H.; Van Berkel, G. J. *Electroanalysis* **1999**, *11*, 857–865.

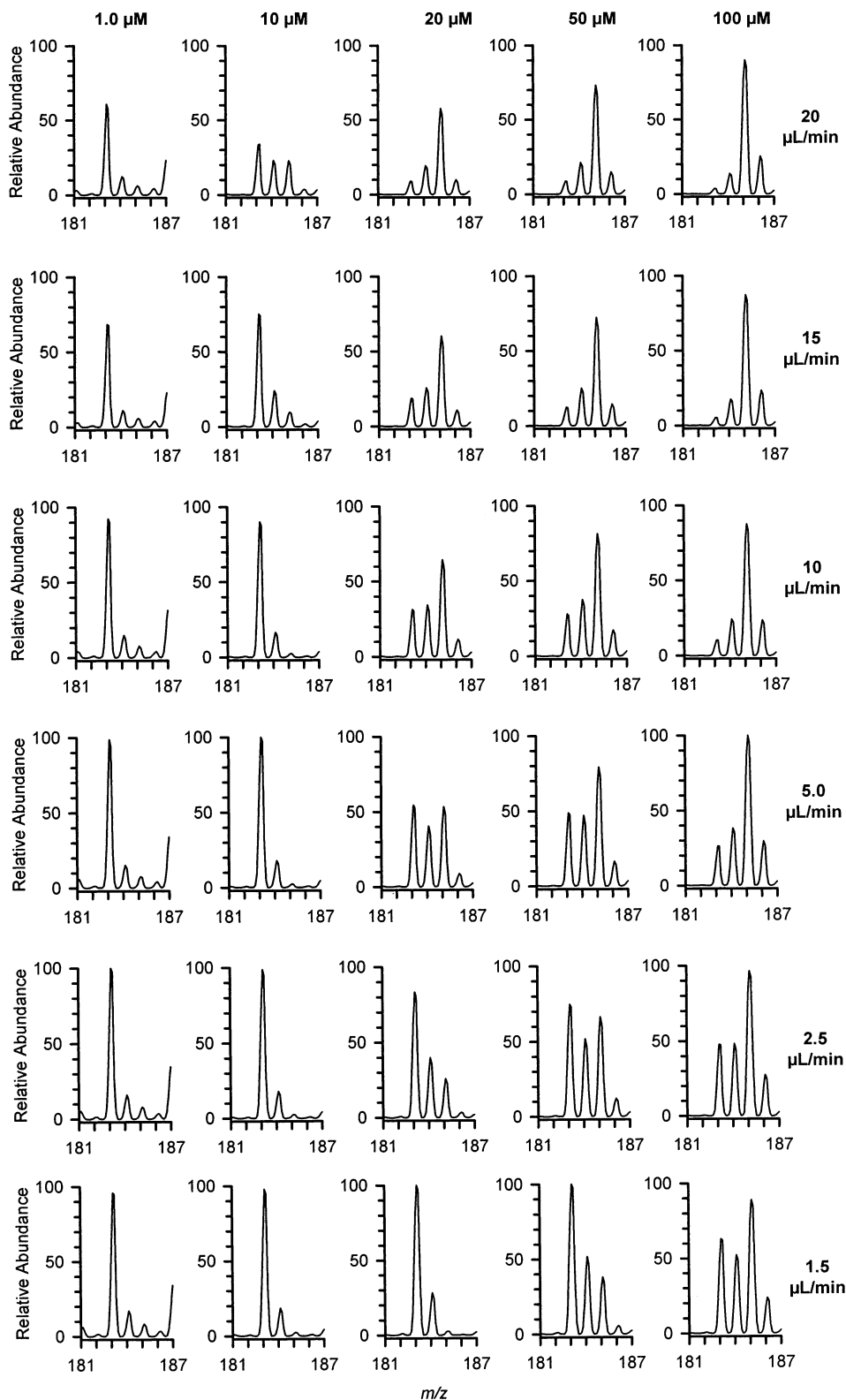


Figure 5. A series of mass spectra showing the molecular ion region for solutions of *N*-phenyl-1,4-phenylenediamine at various concentrations obtained using the planar electrode emitter device with a 6.0-mm-diameter GC electrode at flow rates of 1.5, 2.5, 5.0, 10, 15, and 20  $\mu\text{L}/\text{min}$ . The tip of the emitter spray capillary was placed in the same position for each experiment, and the applied voltage (4.5 kV) and nebulizing gas settings are all identical. Ion abundances are normalized to the largest signal recorded for the molecular species within the data sets for each of the separate solutions analyzed.

among all the electrodes with the thinnest gasket. These results point to the fact that the use of smaller electrodes reduces the efficiency of analyte transport to the electrode and provides one means to limit the extent of analyte modification.

With the 6.0-mm-diameter GC electrode, no material could travel through the cell that did not pass over the face of the electrode. Thus, the maximum mass transport distance in all cases was equivalent to the gasket thickness. With this electrode

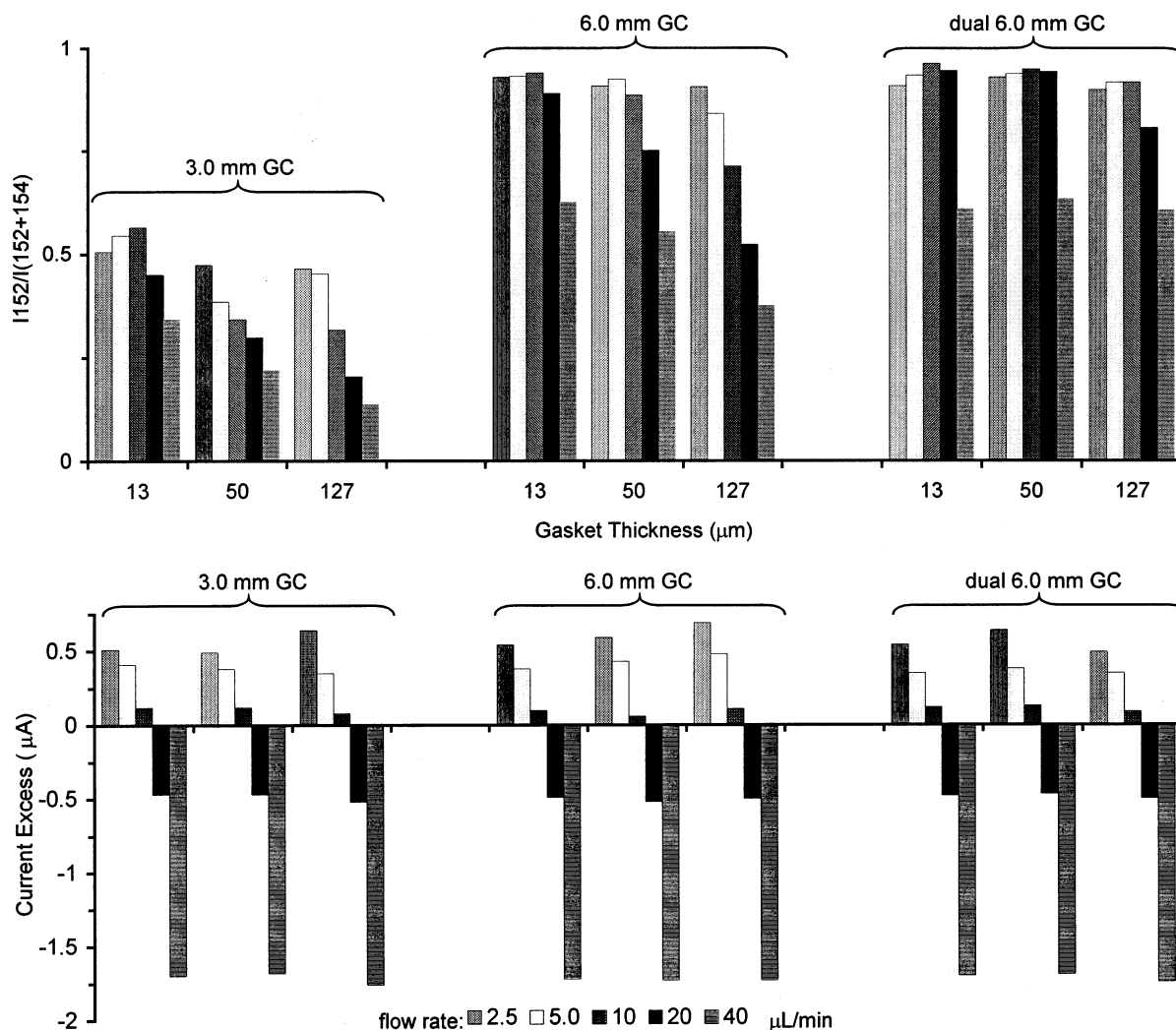


Figure 6. (a) Fraction of the total dopamine in a 20  $\mu\text{M}$  solution (1/1 v/v water/methanol with 5.0 mM  $\text{NH}_4\text{OAc}$  and 0.75% (v) HOAc) oxidized at the emitter electrode plotted as the intensity ratio of peak  $(2 + \text{H})^+$  to the sum of the peaks  $(2 + \text{H})^+$  and  $(2\text{a} + \text{H})^+$  ( $I_{152}/I_{(152+154)}$ ), 1.0 = 100% oxidized; 0 = 0% oxidized) for various electrode sizes, spacing gasket thicknesses, and solvent flow rates. (b) Current magnitude in excess of that required for complete oxidation of the dopamine for the experiments in (a). Negative numbers for current excess indicate insufficient current was measured for complete oxidation.

arrangement, oxidation efficiency increased to  $\sim 90\%$  in the best cases. The narrow 13- $\mu\text{m}$  channel provided for high oxidation efficiency up to  $\sim 20 \mu\text{L}/\text{min}$ , dropping to 60% at 40  $\mu\text{L}/\text{min}$ . When the channel height was increased to 50 and 127  $\mu\text{m}$ , the oxidation efficiency drop off occurred at respectively lower flow rates with increasing channel height and the drop off was more significant. Adding a second 6.0-mm GC electrode in the device, in series with the first, did not further enhance oxidation efficiency for any gasket spacing up to a flow rate of  $\sim 10 \mu\text{L}/\text{min}$ . However, the extent of electrolysis was improved for a flow rate of 20  $\mu\text{L}/\text{min}$  at all gasket spacings, as well as at 40  $\mu\text{L}/\text{min}$  for the two larger spacing gaskets. Improvement in oxidation efficiency by increasing the electrode area would seem to indicate that oxidation can occur a substantial distance along the electrode back upstream, in this case as far as 14-mm (spacing between the two 6-mm-diameter electrodes is 2 mm). At the fast flow rates and with a larger channel height, the analyte may not have enough time on its passage through the device to contact the surface of the single 6.0-mm electrode. By placing another 6.0-mm electrode in the flow stream, the time the analyte is over the electrode (i.e., the

electrolysis time) doubles. Ultimately, however, the ability to completely oxidize the analyte at higher flow rates is limited by the magnitude of the ES current. The data in Figure 6b show that at flow rates of 20 and 40  $\mu\text{L}/\text{min}$  the magnitude of the ES current is well below that required for complete oxidation.

**Membrane-Covered Electrode.** A simple means to eliminate analyte oxidation in ES is to prevent direct contact with the electrode surface.<sup>5,20</sup> This was accomplished with the present device by covering the electrode surface with an ion-permeable membrane. The membrane permits ion transport to and from the electrode through the membrane, but the transfer of organic or biological analytes is hindered relative to other smaller electrolytes in solution ( $\text{NH}_4^+$ ,  $\text{H}^+$ ,  $\text{OAc}^-$ , etc.) that have larger diffusion coefficients.<sup>16</sup> The success of this approach is demonstrated by the data in Figure 7. The same dopamine solution used to acquire the data in Figure 6 was sprayed using the planar electrode emitter at a series of flow rates with and without the membrane covering the 6.0-mm GC electrode. The 127- $\mu\text{m}$  spacing gasket was used

(20) Severs, J. C.; Smith, R. D. *Anal. Chem.* **1997**, *69*, 2154–2158.



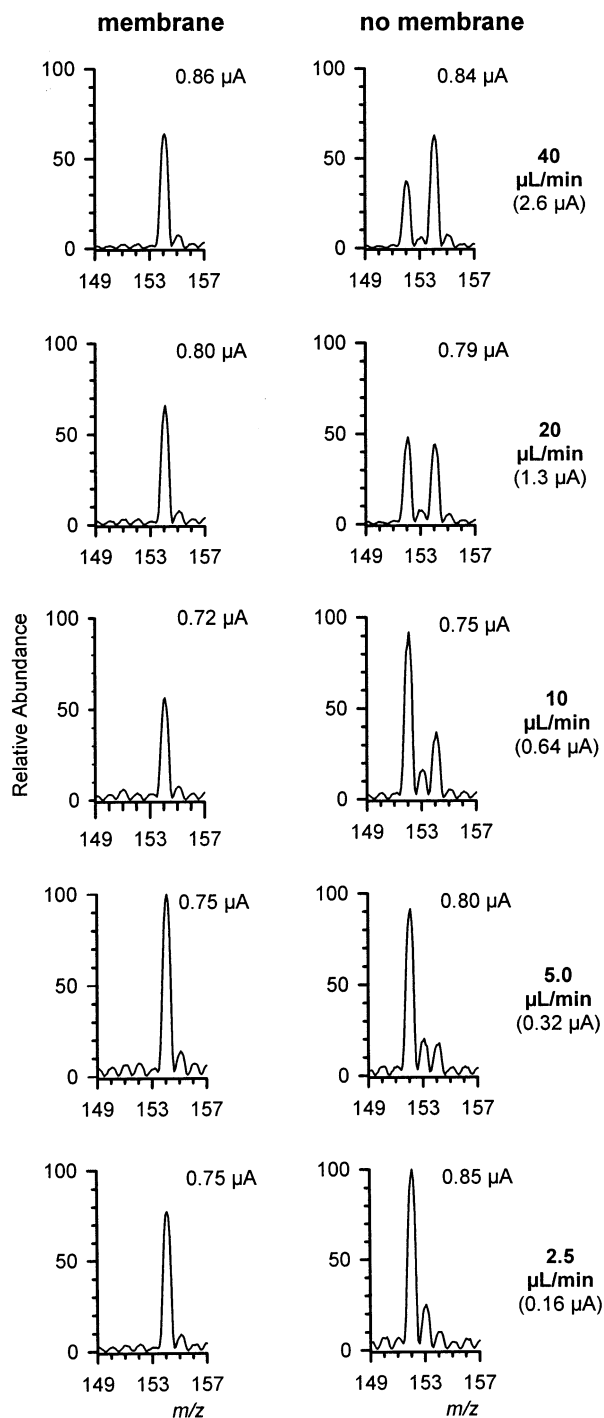


Figure 7. Mass spectra of a 20  $\mu\text{M}$  dopamine solution (1/1 v/v water/methanol with 5.0 mM  $\text{NH}_4\text{OAc}$  and 0.75% (v) HOAc) obtained with planar electrode emitter device utilizing a 6.0-mm-diameter glassy carbon electrode at solvent flow rates of 2.5, 5.0, 10, 20 and 40  $\mu\text{L}/\text{min}$ . The spectra in the left column were obtained with a cellulose ester membrane placed between the electrode and a 127- $\mu\text{m}$  spacing gasket. Spectra in the right column were obtained without the membrane. ES current measured is shown in the respective panels. Current magnitudes in parentheses are those calculated for complete oxidation at the respective flow rates.

for the experiments, because the membrane was compressible and would seal off the flow channel when thinner spacing gaskets were used. One can see that from the highest to lowest flow rates no oxidation of the dopamine was observed with the membrane

in place. However, without the gasket, almost complete oxidation occurred at a flow rate of 2.5  $\mu\text{L}/\text{min}$  and the extent of oxidation was still substantial at 40  $\mu\text{L}/\text{min}$ .

## CONCLUSIONS

The planar electrode ES emitter described here operates with all the capabilities of other ES emitters and with unparalleled versatility for the study and analytical exploitation of the electrochemical processes ongoing at the emitter electrode. Particularly important benefits over tubular electrode emitters in terms of electrochemistry are the wide range of materials that can be used as electrodes and the ability to alter mass transport to the electrode by changes in electrode area or by thin-layer channel height.

With nonelectroactive analytes, the mass spectra obtained with the planar electrode emitter device are very similar to those obtained with our commercial pneumatically assisted ES ion source, which makes use of a stainless steel tubular electrode emitter. With electroactive analytes, the planar electrode system can be used when complete analyte oxidation or when complete avoidance of oxidation is the goal. Easily made changes in electrode area, electrode material, channel height, or solution flow rate can be used to accomplish these opposing tasks. Noncorrodible electrodes such as platinum and glassy carbon, a preferred material in electrochemical studies, should be ideal for oxidation. Corrodible electrodes, including, but not limited to the silver, copper, and zinc electrodes investigated here, can be used as redox buffers. This holds the electrode potential near the equilibrium potential for the respective metal corrosion reactions, thereby avoiding analyte oxidation reactions that require more positive potentials. A byproduct of redox buffering in this way is the introduction of metal ions into solution. In certain scenarios, these metal ions might be the source of chemical noise in a spectrum, but in other cases, they might be used for analytical advantage for the formation of metal-analyte complexes.<sup>15</sup> Another way demonstrated to eliminate analyte oxidation with this device was to cover the electrode with an ion-permeable membrane. This is not a technically feasible option with conductive tubular electrodes, although other ES systems using membranes have been devised that can also limit direct contact with the electrode.<sup>20</sup> Electrodes of different areas can also be used to control the extent of oxidation. Oxidation efficiency generally increases as the area of the electrode increases. Experimental results indicated that oxidation of dopamine might occur upstream along the emitter electrode a minimum of 6 mm and possibly as far back as 14 mm or further.

The discussion and data presented here were limited to positive ion mode ES and oxidation of analytes at the emitter electrode. However, the planar electrode configuration should also benefit the study and use of electrochemical reduction of analytes at the emitter electrode in negative ion mode. Moreover, the basic planar electrode geometry and the relative benefits and caveats for analyte oxidation/reduction discussed here should be directly applicable to lab-on-chip ES systems that use a conductive strip high-voltage electrode contact in the chip microchannel.<sup>21</sup>

(21) Rohner, T. C.; Rossier, J. S.; Girault, H. H. *Anal. Chem.* **2001**, *73*, 5353–5357.

## ACKNOWLEDGMENT

V.K. acknowledges support through an appointment to the Oak Ridge National Laboratory (ORNL) Postdoctoral Research Associates Program administered jointly by the Oak Ridge Institute for Science and Education and ORNL. ES-MS instrumentation was provided through a Cooperative Research and Development Agreement with Sciex (CRADA ORNL96-0458). This research was sponsored by the Division of Chemical Sciences,

Geosciences, and Biosciences, Office of Basic Energy Sciences, U.S. Department of Energy, under Contract DE-AC05-00OR22725 with Oak Ridge National Laboratory, managed and operated by UT-Battelle, LLC.

Received for review April 25, 2002. Accepted July 17, 2002.

AC020267B